RESEARCH ARTICLE

Molecular Reproduction
& Development

Changes in the uterine metabolome of the cow during the first 7 days after estrus

Paula Tríbulo[1,2] | Leandro Balzano-Nogueira[3] | Ana Conesa[3,4] | Luiz G. Siqueira[1,5] | Peter J. Hansen[1,2,4] (ORCID)

[1]Department of Animal Sciences, University of Florida, Gainesville, Florida

[2]D.H. Barron Reproductive and Perinatal Biology Research Program, University of Florida, Gainesville, Florida

[3]Department of Microbiology and Cell Science, University of Florida, Gainesville, Florida

[4]Genetics Institute, University of Florida, Gainesville, Florida

[5]Embrapa Gado de Leite, Juiz de Fora, Brazil

Correspondence
Peter J. Hansen, Department of Animal Sciences, University of Florida, PO Box 110910, Gainesville, FL 32611-0910.
Email: pjhansen@ufl.edu

Funding information
National Institute of Food and Agriculture, Grant/Award Number: 2011-67015-30688; National Institute of Child Health and Human Development, Grant/Award Number: HD088352; LE "Red" Larson Endowment

The uterine microenvironment during the first 7 days after ovulation accommodates and facilitates sperm transit to the oviduct and constitutes the sole source of nutrients required for the development of preimplantation embryos. Knowledge of the composition of uterine fluid is largely incomplete. Using untargeted mass spectrometry, we characterized the uterine metabolome during the first 7 days of the estrous cycle. Bovine uteri were collected on Days 0 ($N = 4$), 3 ($N = 4$), 5 ($N = 3$), and 7 ($N = 4$) relative to ovulation and flushed with Dulbecco's phosphate-buffered saline. A total of 1,993 molecular features were detected of which 184 peaks with putative identification represent 147 unique metabolites, including amino acids, benzoic acids, lipid molecules, carbohydrates, purines, pyrimidines, vitamins, and other intermediate and secondary metabolites. Results revealed changes in the uterine metabolome as the cow transitions from ovulation to Day 7 of the estrous cycle. The majority of metabolites that changed with day reached maximum intensity on either Day 5 or 7 relative to ovulation. Moreover, several metabolites found in the uterine fluid have signaling capabilities and some have been shown to affect preimplantation embryonic development. In conclusion, the metabolome of the bovine uterus changes during early stages of the estrous cycle and is likely to participate in the regulation of preimplantation embryonic development. Data reported here will serve as the basis for future studies aiming to evaluate maternal regulation of preimplantation embryonic development and optimal conditions for the culture of embryos.

KEYWORDS
endometrium, histotroph, maternal-embryo crosstalk, metabolome

1 | INTRODUCTION

The uterus is a dynamic organ that undergoes large-scale changes in morphology and function during the life cycle of the female. This is true for the period encompassing ovulation, mating, and early embryonic development. Coincident with ovulation and mating, the uterus accommodates and facilitates sperm transit to the oviduct (Hawk, 1983). At the same time, the sperm entering the uterus trigger an inflammatory response leading to neutrophil invasion and sperm phagocytosis (Katila, 2012; Schuberth et al., 2008). Antimicrobial defenses in the uterus are also optimal around ovulation (Wira, Fahey, Rodriguez-Garcia, Shen, & Patel, 2014). Following fertilization in the oviduct, the newly formed embryo enters the uterus several days later (4–5 days in the cow; Hackett, Durnford, Mapletoft, & Marcus, 1993) where its survival is dependent on the uterine environment for growth, differentiation,

and placentation. An inadequate uterine environment, such as associated with inflammatory disease (Ribeiro et al., 2016), can lead to embryonic death.

The uterine milieu in which sperm transport, bacterial clearance, and early embryonic development take place is established in large part by secretions from endometrial cells as well as molecules from the blood. Transfer of molecules from the blood to the uterine lumen involves active and selective transport of molecules such as amino acids and specific ions (Fahning, Schultz, & Graham, 1967; McRae, 1988; Schultz, Fahning, & Graham, 1971). In the cow, the species under investigation here, changes in endometrial gene expression (França, da Silva, Pugliesi, Van Hoeck, & Binelli, 2017; Mitko et al., 2008; Tríbulo, Siqueira, Oliveira, Scheffler, & Hansen, 2018), and protein secretion (Malayer, Hansen, & Buhi, 1988) during the first 7–8 days after estrus have been reported. There is also some information about changes in the presence of small molecules present in the uterine fluid during this period, especially for amino acids (Fahning et al., 1967; França et al., 2017; Hugentobler et al., 2007; Roussel & Loe, 1973) and select ions and sugars (Hugentobler et al., 2010; Schultz et al., 1971).

The objective of the present study was to characterize the metabolome of the lumen of the uterus of the cow during the first 7 days after ovulation. It was hypothesized that the uterine metabolome changes during the first 7 days after ovulation to meet the changing role of the uterus in sperm transport, immune defense, and early embryonic development. A second objective was to identify metabolites in uterine fluid during this time known to affect preimplantation embryonic development. Such molecules might be useful targets for efforts to improve cow fertility or for addition to culture media in systems for in vitro production of embryos.

2 | MATERIALS AND METHODS

2.1 | Synchronization of the estrous cycle

Nonlactating Holstein cows were also used for a previously reported study (Tríbulo et al., 2018). A total of 20 cows with a detectable corpus luteum as determined by transrectal ultrasonography were subjected to a hormonal protocol to synchronize ovulation. On Day 18 (day of expected ovulation = Day 0), cows were injected, intramuscular, with 25 mg prostaglandin (PGF, Lutalyse®; Zoetis, Florham Park, NJ) followed by 100 µg gonadorelin (GnRH, Cystorelin®; Merial Inc., Duluth, GA) on Day 16. A second, identical injection of GnRH was given on Day 9 and a progesterone-containing controlled internal drug release device (CIDR®; Zoetis) was inserted intravaginally. Subsequently, at Day 4, each cow was given PGF (25 mg, im), and the intravaginal device was removed. Another 25 mg PGF was injected at Day 3 and 100 µg GnRH was injected intramuscularly at Day 2, that is, 24 hr after PGF. Transrectal ultrasonography of ovaries was performed on Days -4, -1, and 0 to confirm ovulation. A total of 15 cows were successfully synchronized and were slaughtered at Day 0 ($n = 4$), 3 ($n = 4$), 5 ($n = 3$), or 7 ($n = 4$) relative to the expected day of ovulation.

2.1.1 | Uterine flushings

Reproductive tracts were obtained immediately after slaughter and placed on ice. Processing of all organs was completed within 4 hr. The side of the reproductive tract was identified as being ipsilateral or contralateral to the side of ovulation. Ovulation of cows slaughtered at Day 0 was confirmed by the absence of a preovulatory follicle in three of four cows. For the remaining cow, ovaries were lost during processing and ovulation could not be confirmed.

Mesometrium was removed and the uterine horn ipsilateral to the site of ovulation was clamped near the uterine body. The oviduct was removed by cutting it at the uterotubal junction. The uterine wall in this opening was handled with two hemostats to guide the opening to a 50 ml tube (Sarstedt AG & Co., Numbrecht, Germany). Using an 18-Ga needle, 30 ml of Dulbecco's phosphate-buffered saline at room temperature were flushed into the uterine horn from the end near the clamp and the fluid propelled by massage along the uterine horn through the opening at uterotubal junction. Recovered fluid was kept in ice. After centrifugation at 3,000g for 15 min at 4°C, the supernatant fraction was obtained and stored at −20°C.

2.2 | Metabolomics

Metabolites present in uterine flushings from the side ipsilateral to ovulation were identified by liquid chromatography and mass spectrophotometry (LC–MS) at the Southeast Center for Integrated Metabolomics at the University of Florida. Analyses were performed on a Thermo Q-Exactive High Resolution Mass Spectrometer coupled with a Dionex UHPLC and autosampler (Thermo Fisher Scientific, Waltham, MA). The instrument runs both positive and negative ion modes with heated electrospray ionization. Mass resolution was 70,000 at m/z 200 with mass accuracy of <5 ppm in positive mode and <10 ppm in negative mode. Separation of metabolites was achieved on an Ace C18-PFP column (100 × 2.1 mm, 2 µm; Advanced Chromatography Technologies, Aberdeen, Scotland) with 0.1% (vol/vol) formic acid in water as mobile phase A and acetonitrile as mobile phase B and with a column temperature of 25°C.

Samples were prepared by mixing 100 µl of each thawed uterine fluid sample with 20 µl of internal standard mix (creatine-D3, L-leucine-D10, L-tryptophan-D3, and caffeine-D3) and 800 µl of 8:1:1 acetonitrile:methanol:acetone (vol/vol/vol) solution. Samples were then vortexed for 10 min and cooled in a refrigerator for 30 min. The tubes were centrifuged at 20,000g for 10 min to pellet the protein. The supernatant was then transferred to a new tube and dried down with nitrogen. The dried material was reconstituted by adding 100 µl of 0.1% (vol/vol) formic acid in LC–MS grade water.

The flow rate was set to 350 µl/min with a total run time of 20 min. A total of 2 µl of each sample was injected for positive ion mode analysis and 4 µl was injected for negative ion mode analysis. The LC–MS data were processed using MZmine 2 software (Pluskal, Castillo, Villar-Briones, & Orešič, 2010) for peak picking and alignment, and for generation of intensity tables for statistical analyses. MZmine (freeware; http://mzmine.github.io/) was used to

identify features, deisotope, align features and perform gap filling to fill in any features that may have been missed in the first alignment algorithm. All sodiated or potassiated adducts of the protonated ion and dimer or trimer complexes of the same ion were identified and removed from the data set. Metabolites were first identified by use of an in-house curated retention time metabolite library (Ulmer, Yost, Chen, Mathews, & Garrett, 2015). Subsequently, additional external databases such as the human metabolome database (www.hmdb.ca) were used to expand the number of identified metabolites.

2.2.1 | Statistical analysis

Multivariate analysis was performed in Metaboanalyst (version 3.0; http://old.metaboanalyst.ca/MetaboAnalyst/ Xia & Wishart, 2016) using partial least-squares discriminant analysis (PLS-DA) evaluating positive and negative ion data separately. The data were sum-normalized, log-transformed, and autoscaled before PLS-DA analysis. The 184 features with putative identification were also subjected to analysis of variance using the GLM procedure of SAS for Windows, version 9.4 (SAS Institute Inc., Cary, NC) with the day as a fixed effect in the statistical model. Orthogonal contrasts were calculated to identify the pattern of variation over days, including linear, quadratic, and cubic effects of the day. For analysis of variance, data were log transformed to meet the assumptions of the normal distribution. Least-squares means were back-transformed and SEM calculated as outlined by Jørgensen and Pedersen (1998). Level of significance was established at $p < 0.05$ and the statistical tendency was considered when $0.05 > p < 0.10$.

A canonical analysis of populations (CAPs) was performed upon merging positive and negative data sets. The CAP is a methodology based on the Mahalanobis distance that uses a linear combination of predictor variables to identify new canonical components that maximize the variability among groups relative to the variability within group while maximizing the following function:

$$g(v) = \frac{v^T H_v}{v^T S_v},$$

where v is a vector of values that maximizes the variability of the vector of original variables; v^T is the transpose of v, H_v is the covariance matrix among groups, and S_v is the covariance matrix within groups. Thus, $g(v)$ is a relationship between variance among groups (numerator) and variance within groups (denominator) imposing the latter as equal to 1 (Amaro, Vicente-Villardón, & Galindo-Villardón, 2004; Krzanowski, 1989). Using this approach, statistically significant variables ($p < 0.05$) were retained and used for graphing.

3 | RESULTS

3.1 | Characteristics of identified molecules

There were a total of 1,419 features detected in the positive ion mode and 574 features in the negative ion mode. Of these, identification was established for 108 peaks in the positive mode and 76 peaks in the negative ion mode (Supporting Information Table S1). Those 184 peaks with putative identification represent 147 unique metabolites.

Features identified in the negative and positive ion modes were classified into 10 superclasses, 25 classes, and 38 subclasses based on the human metabolome database (http://www.hmdb.ca). Superclasses represented by features assigned a metabolite were: benzenoids; inorganic compounds; lipids and lipid-like molecules; nucleosides, nucleotides, and analogues; organic acids and derivatives; organic nitrogen compounds; organic oxygen compounds; organoheterocyclic compounds; organooxygen compounds and phenylpropanoids and polyketides. Subclasses represented by features assigned a metabolite are listed in Supporting Information Table S2.

All metabolites were present on all days. The peak intensity (i.e., proportional to the concentration) of the features identifying these metabolites, however, varied across time. The total intensity of identified features for each subclass of metabolite on Days 0, 3, 5, and 7 relative to ovulation was estimated by dividing the sum of intensities of identified features within a subclass by the sum of intensities of all 184 identified features. Results are shown in Figure 1. The most abundant subclass of metabolites at all times was the amino acids, peptides, and analogues subclass. A total of 52 features were assigned to this subclass, with tryptophan, tyrosine, phenylalanine, leucine, and aspartic acid being within the five to seven most abundant amino acids for each day.

The second most abundant subclass of metabolites present in the uterine fluid for Days 0 and 5 was benzoic acids and derivatives, with hippuric acid representing 96% of the total intensity of metabolites in this category. For Days 3 and 7, the second most abundant subclass of metabolites was carbohydrates and carbohydrate conjugates. Citric acid, glyceraldehyde lactate, and glucose or fructose were the most abundant metabolites of the carbohydrates and carbohydrates conjugates at all days. Glyceraldehyde lactate was the most abundant metabolite in this subclass at Days 0 and 5, representing 56.0% and 48.7%, respectively, of the total intensity of metabolites for the subclass. On Days 3 and 7, citric acid was the predominant metabolite for this subclass representing 54.4% and 52.9%, respectively, of the total intensity of metabolites for the subclass.

A total of seven fatty acids were detected. Among the most abundant were 3-tert-butyladipic acid, methyladipic acid, deoxycarnitine, and isobutylcarnitine. There were five purines and four pyrimidines detected. Urate was predominant on Days 0 and 5 constituting 81.2% and 84.5% of the purine subclass, respectively. Hypoxanthine was predominant on Days 3 and 7, constituting 53.8% and 77.1% of the purine subclass, respectively. Pyrimidines were mainly represented by uracil on Days 0 and 7, constituting 57.6% and 51.8% of the subclass. Dihydrouracil was abundant as well, constituting 29.9%, 29.2%, 41.9%, and 30.3% on Days 0, 3, 5, and 7, respectively. Isocytosine represented 35.0% of the pyrimidines in uterine fluid on Day 3 but was lower than 15% of the pyrimidines at the other times.

Subclasses that contained only one to three metabolites were grouped together and denominated "others." Choline was within the
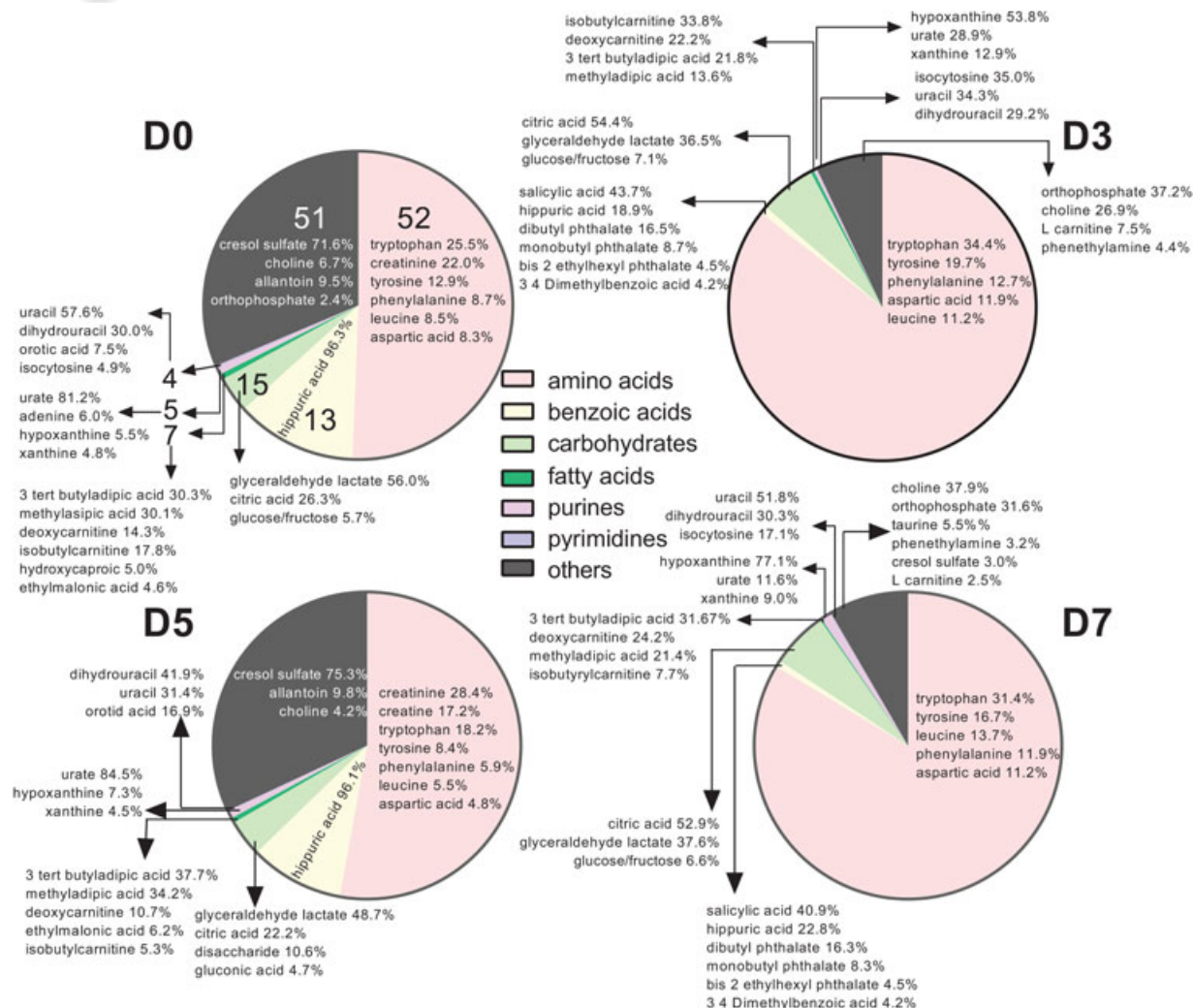
FIGURE 1 Pie graph representing the proportion of identified metabolites in uterine flushings assigned to specific subclasses of the human metabolome data set. Each pie represents the sum of intensities of identified metabolites within a subclass as a percent of the sum of intensities of all 184 identified features for Day 0 (D0), Day 3 (D3), Day 5 (D5), and Day 7 (D7) relative to ovulation. Numbers on each pie slice for Day 0 represent the total number of metabolites identified for each subclass (number of metabolites per subclass were the same for each day). The group referred to as "others" includes subclasses with 1–3 metabolites. The percent data within each slice indicates the proportion of the total intensity in a subclass (i.e., sum of all intensity peaks for each subclass) represented by a given metabolite [Color figure can be viewed at wileyonlinelibrary.com]

top three to six most abundant molecules on all days and represented up to 37.9% of the total intensity of molecules of this category. Although not abundant on Day 3 or 7, cresol sulfate represented 71.6% and 75.3% of the total intensity of molecules of this category on Days 0 and 5, respectively. Orthophosphate represented 37.2% and 31.6% of the total intensity of molecules of this category on Days 3 and 7, respectively.

3.2 | Use of multivariate analyses to discriminate between days relative to ovulation

Results are shown in Figure 2. The PLS-DA showed separation of the data with Component 1 and Component 2 describing 60.6% (positive mode; Figure 2a) and 61.3% (negative mode; Figure 2b) of the variance. There was less variation among samples on Day 7 than on other days. Moreover, there was partial overlap

in the characteristics of the metabolome on Days 0, 3, and 5. The permutation test for PLS-DA results yielded a p value of 0.019 (positive mode) and 0.015 (negative mode) for two components.

CAPs also yielded statistically significant separation of uterine metabolomes according to the day relative to ovulation (Figure 2c,d). Results showed that all 4 days were well described using three canonical variables. The first canonical variable retained 60.9% of the variance, the second retained 28.7% and the third variable retained 10.4% of the variance. Centroids and confidence interval ellipses (95%) were calculated using individuals. The groups with confidence ellipses that do not overlap between each other are significantly different. By this criterion, the metabolome on Day 0 differs from Days 3, 5, and 7; Days 3 and 5 are similar to each other (differences not captured in canonical variables 1 or 2 but captured in canonical variable 3); and Days 3 and 5 were different from Day 7. When
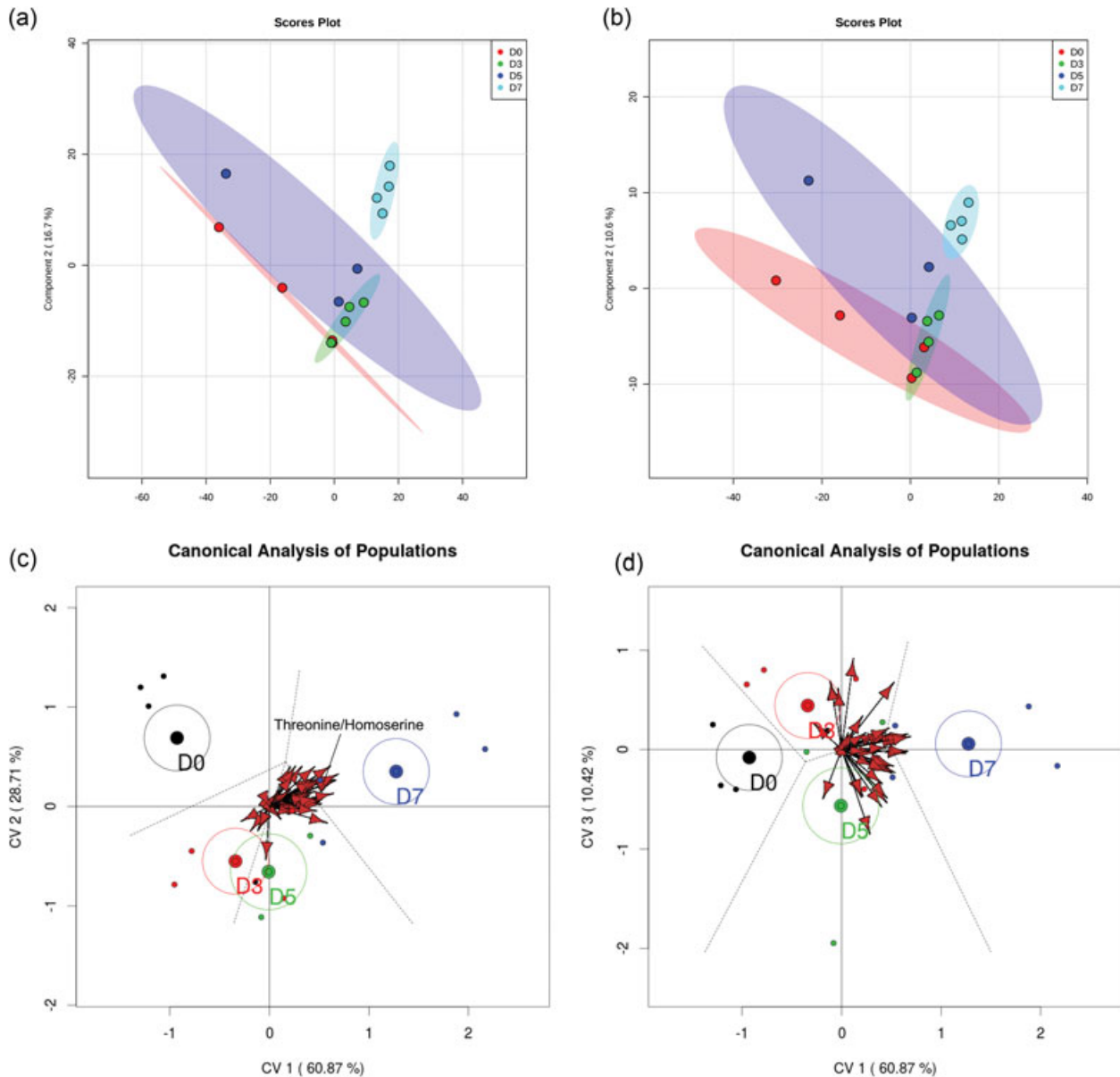
FIGURE 2 Partial least-squares discriminant analysis (PLS-DA). (a, b) The PLS-DA of the positive (a) and negative (b) data sets including all features while (c and d) are biplot representations of a canonical analysis of populations from merged positive and negative data sets. (c) The relationship between canonical variables 1 and 2. (d) The relationship between canonical variables 2 and 3. Vectors represent statistically significant ($p < 0.05$) features across days relatives to ovulation. The vectors point towards the day in which intensity of the feature increases and length of the vector reflects the magnitude of variance explained by that feature. One vector, for threonine/homoserine, is labeled for illustrative purposes [Color figure can be viewed at wileyonlinelibrary.com]

looking at the canonical variable 3, which explains 10% of the variation, Days 3 and 5 are separated.

There were 46 statistically significant variables represented by vectors in the plot (Figure 2c,d); their correlation with the canonical variables were studied to determine their relationship with the day relative to ovulation. Only 10 of the 46 variables have a putative identification, representing seven unique metabolites. In order of significance, those metabolites were threonine/homoserine, uridine, hypoxanthine, methionine sulfoxide, D-ribose, L-glutamine, and glutathione disulfide. The complete list of significant metabolites, with their respective relative quality of representation related to

each canonical variable, is available in Supporting Information Table S3.

3.3 | Analysis of variance to identify molecules whose intensity changed with day relative to ovulation

Of the features with a designated identity, there were a total of 39 in the positive mode and 19 in the negative mode that were affected by day (Supporting Information Table S4). An additional 15 features in the positive mode and 14 in the negative mode tended to be affected

6C-Sugar alcohol

Isobutyrylcarnitine

Proprionylcarnitine
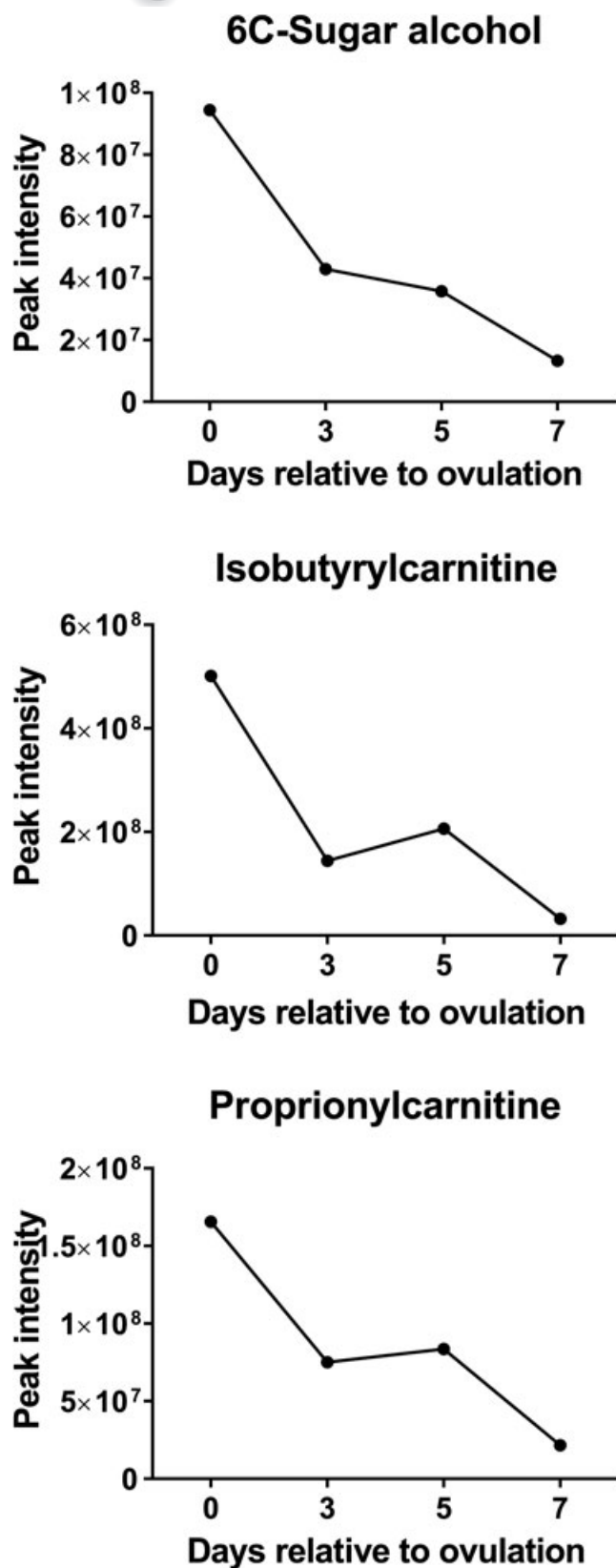
FIGURE 3 Changes in concentration during the first 7 days after ovulation for molecules where the intensity decreased from Days 0 to 7 relative to ovulation ($p < 0.05$). Data are least-squares means. p values for linear, quadratic, and cubic effects of day and the *SEM* are reported in Supporting Information Table S4. *SEM*, standard error mean

by day. A total of 12 metabolites that changed or tended to be affected by day were identified twice based on different features. Except for one case (taurine), in each of the 12 cases, the same pattern of change was seen for both features.

Changes of the intensity of the features significantly affected by day were characterized by four different patterns. In the first pattern, represented by isobutyrylcarnitine, proprionylcarnitine, and 6C-sugar alcohol, there was a linear decrease from Days 0 to 7 (Figure 3). The second pattern, represented by guanine, hypoxanthine, methionine sulfoxide, orthophosphate, phenethylamine, threonine/homoserine, and uridine, was characterized by little change in intensity from Days 0 to 3 and an increase from Days 3 to 7 (Figure 4). The third pattern, represented by 14 metabolites, was a decrease in intensity from Days 0 to 3 and then an increase from Days 3 to 7. Metabolites in this group were 2-hydroxyphenylalanine, aspartate, D-ribose, glycerol, glycine, isocystosine, leucylproline, leucine, L-glutamine, L-tyrosine, polyethylene glycol n5 (PEG n5), taurine, urate, and xanthine (Figure 5). Finally, the pattern with the most metabolites represented was characterized by a decrease in intensity from Days 0 to 3, and increase to a maximum intensity on Day 5, and a decrease thereafter on Day 7. Metabolites following this pattern were 3-(2-hydroxyphenyl) propanoate, 3,4-dihydroxybenzenesulfonic A, 4-acetamdobutanoate, 4-hydroxybenzenesulfonic acid, 5,6-dihydrouracil, aldopentose, allantoin, α-aminoadipate/N-methyl-L-arcosine/β-alanine, betaine, choline, creatine, cytidine, guanidinoacetate, hippuric acid, homovanillate, hydroxyhippuric acid, L-kynurenine, L-methionine, N(pai)-methyl-L-histidine, N-acetyl-L-aspartic acid, N-acetylputrescine, N-α-acetyl-L-lysine, N-methyl-L-glutamate, phosphor(enol) pyruvic acid, uracil, and p-cresol sulfate (Figure 6).

3.4 | Molecules identified in uterine flushings with known role in cell signaling

Thirty-one unique metabolites (revealed by 36 features) possess a known signaling function (Table 1). Among these metabolites, there were amino acids, intermediate metabolites of oxidative respiration and amino acid metabolism. Of the metabolites with signaling function, L-glutamine, methionine sulfoxide, and phenethylamine changed during the first 7 days relative to ovulation ($p < 0.05$). In particular, these three metabolites increased from Days 3 to 7 (Figures 4 and 5). In addition, 4-acetamidobutanoate, α-aminoadipate, choline, L-kynurenine, N-acetyl-L-aspartic acid, N-α-acetyl-L-lysine, N-methyl-L-glutamate, and p-cresol sulfate changed during the first 7 days relative to ovulation with maximum intensity occurring on Day 5 ($p < 0.05$; Figure 6).

3.5 | Molecules identified in uterine flushings with reported role in regulation of embryonic development

Of all features with a putative ID, there were 14 metabolites (identified with a total of 20 features) that have been reported to affect preimplantation embryonic development in either the cow or
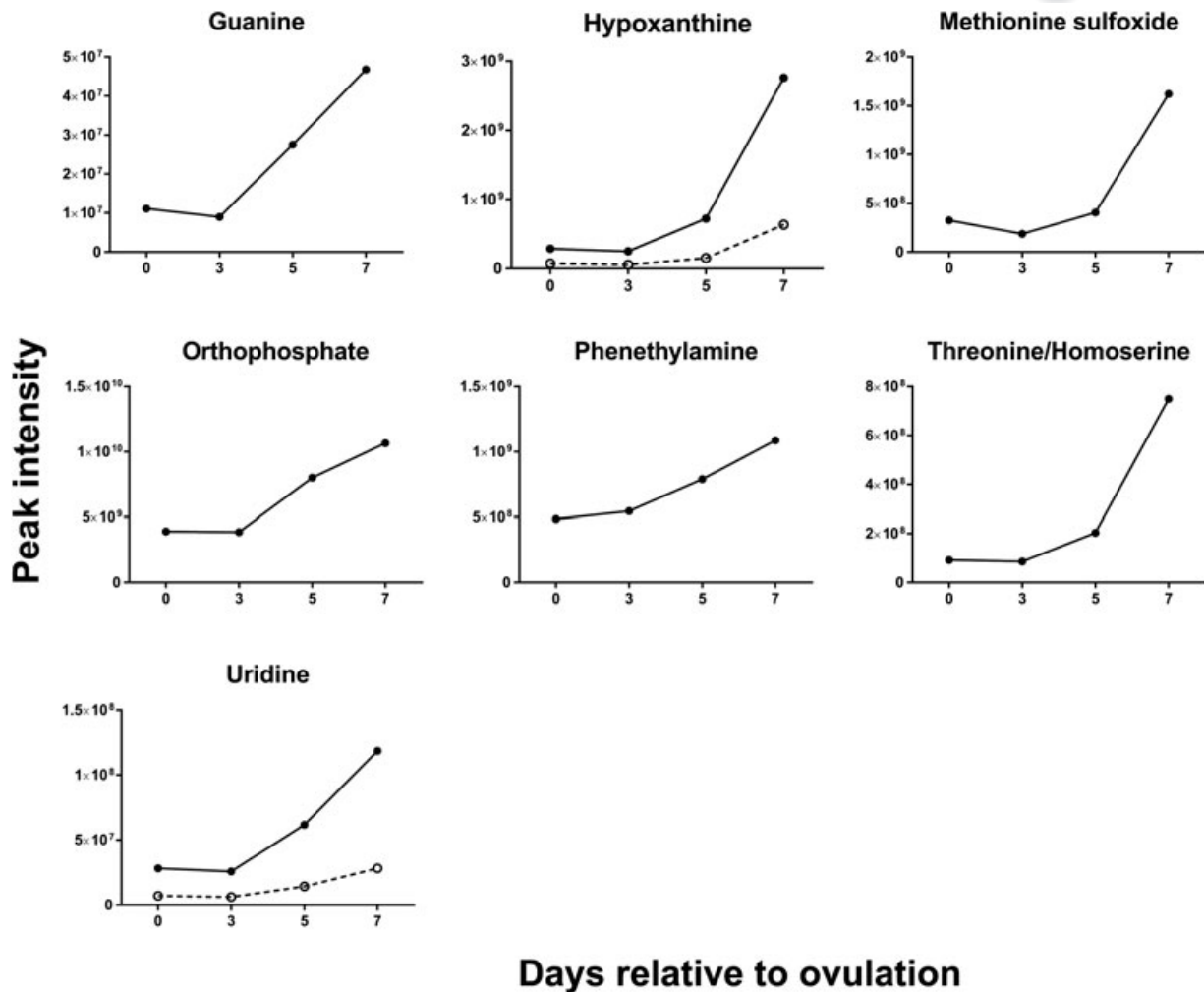
FIGURE 4 Changes in concentration during the first 7 days after ovulation for molecules where the intensity was similar at Days 0 and 3 but then increased from Days 3 to 7 relative to ovulation ($p < 0.05$). Metabolites with more than one feature are indicated by two lines. Data are least-squares means. p values for linear, quadratic, and cubic effects of day and the *SEM* are reported in Supporting Information Table S4. *SEM*, standard error of the mean

one or more other mammals (Table 2). Three of the metabolites were phthalates which could have been introduced into the flushings from the plastic tubing used for fluid collection. Four metabolites (*N*-methyl-L-glutamate, taurine, leucine, and L-methionine) changed during the first 7 days relative to ovulation. Leucine and taurine increased linearly from the day of ovulation to Day 7 (Figure 5) whereas *N*-methyl-L-glutamate and L-methionine decreased from Days 0 to 3, peaked on Day 5 and decreased by Day 7 ($p < 0.05$; Figure 6).

4 | DISCUSSION

This paper is one of the first reports to characterize the metabolome of the uterine lumen of any mammalian species (Romero, Liebig, Broeckling, Prenni, & Hansen, 2017). As expected, the composition of the uterine lumen varied with time, with large differences between the metabolome on Days 0 and 7 and with Days 3 and 5 being

intermediate. These changes accompany alterations in the endocrine regulation of the uterus, from an organ regulated by estrogen on Day 0 to one dominated by actions of progesterone on Day 7. In addition, changes in the metabolome are coincident with changes in the function of the uterus from one of postmating sperm transport and bacterial removal on Day 0 to support for development of the embryo on Days 5 and 7. Many of the metabolites found in the uterus are known to regulate cell signaling or have been reported to affect embryonic development. These may be important molecules for survival of the embryo in vivo and in vitro.

Modifications in the constituents of the uterine metabolome from Days 0 to 7 after ovulation probably reflect, in part, hormone-driven changes in vascular blood flow and permeability. Estrogen can increase endometrial edema and this action is likely to involve increased blood flow (Koos, 2011) as well as paracellular leakage of the endothelium because of reduced formation of tight junctions (Aberdeen, Wiegand, Bonagura, Pepe, & Albrecht, 2008; Hata et al., 2014). One mechanism by which estradiol increased vascular
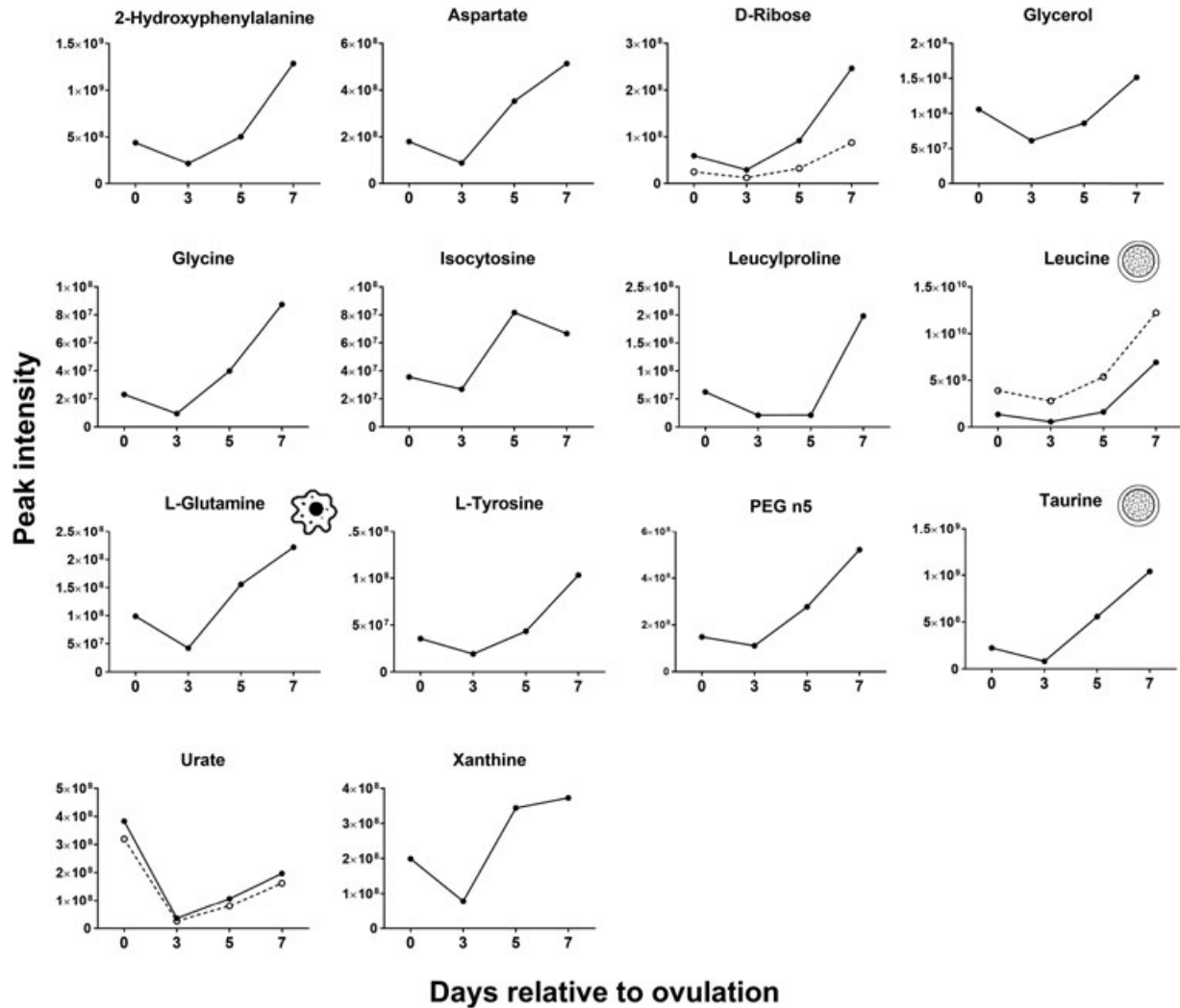
FIGURE 5 Changes in concentration during the first 7 days after ovulation for molecules where the intensity decreased from Days 0 to 3 and then increased from Days 3 to 7 relative to ovulation ($p < 0.05$). Metabolites with more than one feature are indicated by two lines. Icons placed within individual graphs indicate that the metabolite has been reported to activate one or more cellular signaling pathways (cell icon) or to affect preimplantation embryonic development (morula icon). Data are least-squares means. p values for linear, quadratic, and cubic effects of day and the *SEM* are reported in Supporting Information Table S4. *SEM*: standard error of the mean

permeability is through increased endometrial synthesis of vascular endothelial growth factor (Albrecht et al., 2003). Progesterone also increases vascular permeability (Goddard et al., 2014). In the cow, timed-average maximum velocity of blood flow through uterine arteries was greater on Day 1 relative to ovulation than on Day 7 after ovulation (Bollwein, Prost, Ulbrich, Niemann, & Honnens, 2010) but there were no differences in measurements of blood flow in uterine arteries between Days 3 and 6 after estrus (Honnens et al., 2008).

Another mechanism by which steroids can regulate the composition of the metabolome is through regulation of secretory activity of endometrial cells. Concentrations of amino acids in uterine fluid were largely greater than concentrations in blood serum (Fahning et al., 1967). In the cow, supplementation with progesterone increased endometrial expression of the amino acid transporter genes *SLC1A1*, *SLC1A4*, *SLC7A1*, *SLC7A7*, *SLC38A7* , and *SLC43A14* on Day 7 of the

estrous cycle while decreasing expression of *SLC1A5* (Forde et al., 2014). Similarly, manipulation of follicular growth to produce a large ovulatory follicle increased endometrial expression of *SLC6A6*, *SLC7A4*, *SLC17A5*, *SLC38A1*, and *SLC38A7* on Day 4 of the estrous cycle (França et al., 2017). These transporters mediate transport of aspartic acid, glucose, glutamate, leucine, and taurine that were found in abundant quantities in the present study.

Multivariate analysis indicated that the metabolome on Days 0, 3, and 5 were more similar to each other than the metabolome on Day 7. Moreover, there were only three metabolites that were highest in intensity on Day 0 as compared to other days but there were 20 metabolites that had highest intensity on Day 7. One possible interpretation of this result is that the metabolome is programmed to change in composition to meet the needs of the developing embryo, which first enters the uterus on Days 4–5 after ovulation (Hackett et al., 1993) but does not need to be
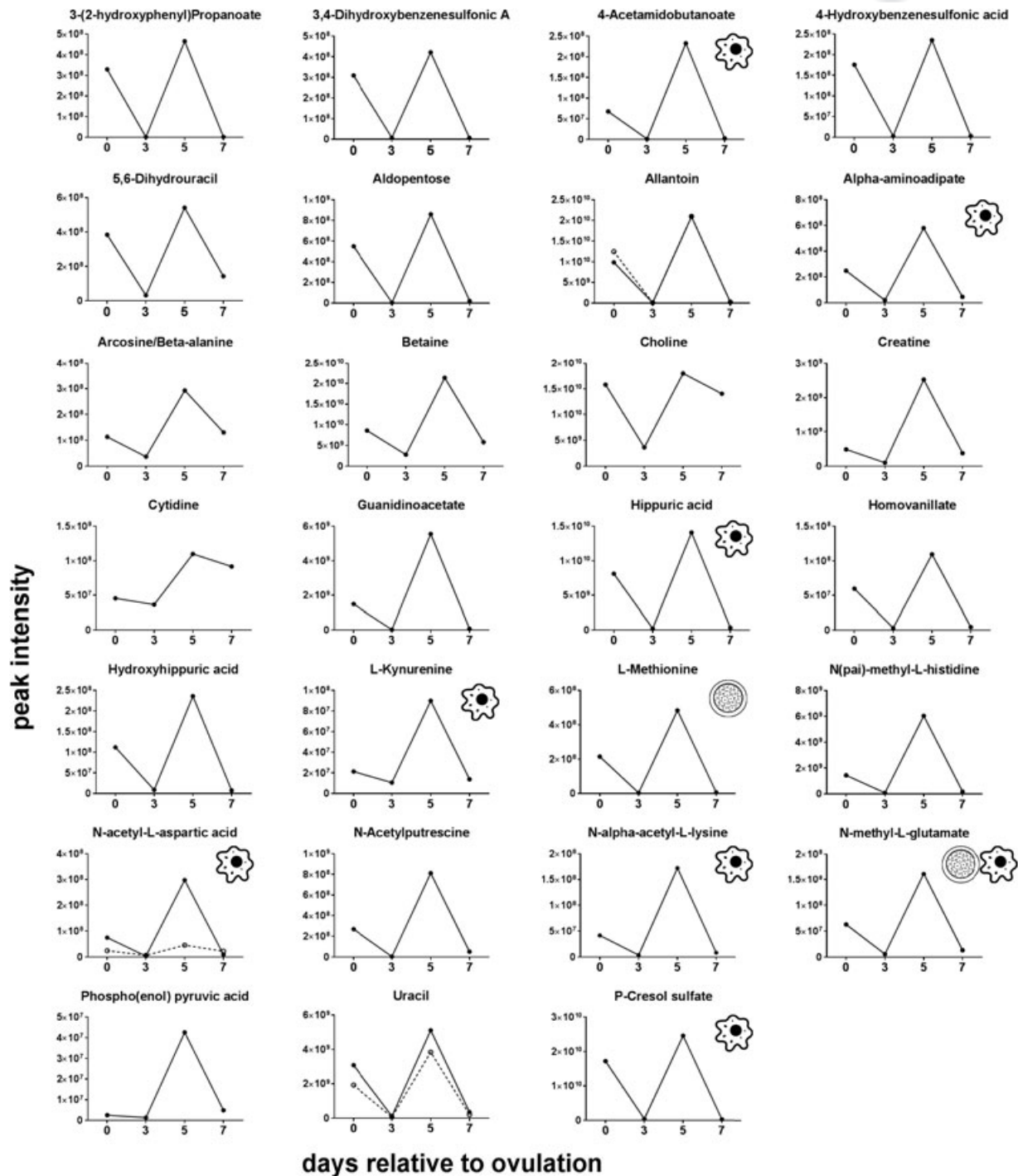
FIGURE 6 Changes in concentration during the first 7 days after ovulation for molecules where the intensity decreased from Days 0 to 3, increased to a maximum on Day 5 relative to ovulation, and decreased afterwards ($p < 0.05$). Metabolites with more than one feature are indicated by two lines. Icons placed within individual graphs indicate that the metabolite has been reported to activate one or more cellular signaling pathways (cell icon) or to affect preimplantation embryonic development (morula icon). Data are least-squares means. p values for linear, quadratic, and cubic effects of day and the *SEM* are reported in Supporting Information Table S4. SEM: standard error of the mean

preprogrammed to allow for sperm transport or bacterial removal coincident with mating on Day 0. Perhaps, the uterine metabolome does not need to change greatly to allow sperm to survive in the uterus or for the inflammatory responses associated with semen deposition to occur. It may also be that sperm transport or bacterial removal is facilitated by concentrations of specific metabolites being low. Interestingly, two of the three metabolites found to have greatest intensity on Day 0, isobutyrylcarnitine and proprionylcarnitine, increase in intensity at the uterotubal junction during sperm storage in the tropical bat, *Scotophilus heathi* (Roy & Krishna, 2013). It

TABLE 1 Metabolites with a potential signaling function that were present in flushings from the uterine horn ipsilateral to the side of ovulation within the first 7 days relative to ovulation

Putative identification
Cysteine sulfinate
4-Oxoproline
Kynurenic acid
L-Glutamic acid
L-Glutamine
N-Acetylaspartylglutamic acid
N-Acetyl-L-aspartic acid
N-Acetyl-L-leucine
Orotic acid
p-Cresol sulfate
Succinate
Succinic acid-13C4
Urocanate
2′,4′-Dihydroxyacetophenone
4-Acetamidobutanoate
4-Aminobutanoate (GABA)
5-Hydroxymethyl-2-furaldehyde
5-Oxo-L-proline/pyroglutamic acid
α-Aminoadipate/N-methyl-L-glutamate
Choline
Diethanolamine
Guanidinoacetate
Kynurenic acid
L-Glutamine
L-Proline
L-Valine/5-aminopentanoate/L-norvaline
Methionine sulfoxide
N-acetyl-L-aspartic acid
N-α-acetyl-L-Lysine
Noradrenaline
Phenethylamine
Proprionyl-L-carnitine
Stachydrine
Succinate
Triethyl phosphate
Urocanate

is also possible that additional metabolites important for uterine events accompanying semen deposition accumulate in the uterine lumen as part of the inflammatory response to sperm.

The potential importance of specific constituents of the uterine metabolome for optimal development of the embryo is indicated by two findings. First, embryos produced in vitro, in the absence of most of the molecules ordinarily present in the uterine lumen, have a wide array of abnormal phenotypes (Hansen, Block, Loureiro, Bonilla, & Hendricks, 2010). Such disordered development could be a consequence of absence of critical regulatory or nutritive molecules. Second, a large number of molecules identified in the metabolome of the uterine lumen have been reported to regulate embryonic development (excluding phthalates, $n = 11$) or affect cell signaling more generally ($n = 31$). Most of the molecules reported to affect embryonic development did not change in intensity with days after ovulation. However, leucine and taurine had highest intensity on Day 7 and N-methyl-L-glutamate and methionine was highest on Day 5. N-methyl-L-glutamate has been reported to increase developmental competence to the blastocyst stage in the rat (Nakamura et al., 2016). Taurine has similar actions in the rat (Nakamura et al., 2016) and cow (Ealy, Drost, Barros, & Hansen, 1992), and feeding of methionine increased lipid content and reduced DNA methylation in embryos produced by superovulation (Acosta et al., 2016). In the rabbit preimplantation embryo, leucine can activate mammalian target of rapamycin (mTOR) signaling and increase expression of genes involved in cell cycle, proliferation, translation, and amino acid transport (Gürke et al., 2016). Leucine also activates mTOR signaling in the mouse preimplantation embryo and has been implicated in activation of changes in the trophoblast leading to implantation (González et al., 2012).

Among the categories of metabolites present in the uterine lumen, that of amino acids, peptides, and analogues were the most abundant type of molecule at each day examined. In contrast to few reports on uterine concentration of amino acids at similar times of the estrous cycle, in which the most abundant amino acids were glycine, taurine, and alanine (Elhassan et al., 2001; Fahning et al., 1967; Hugentobler et al., 2007) or threonine, arginine, and glutamic acid (Roussel & Loe, 1973), the most abundant amino acids found in our study included tryptophan, tyrosine, phenylalanine, and leucine. It is worth noticing that the aforementioned studies did not flush the uterus. These methodological methods may be responsible for the discrepancy in the results.

Only seven fatty acids were identified in our study. It might be expected that metabolomics analysis using mass spectrometry in the present study would identify more lipids and lipid derivatives, especially when compared to the characterization of a large number of phospholipids in the bovine uterine lumen (Belaz et al., 2016). In the study of Belaz et al. (2016), ionization of the samples before MS was performed using a matrix-assisted laser desorption/ionization, a technique that minimizes molecule fragmentation during this ionization. In addition, only a small fraction of the features identified in the current study were assigned a metabolite and an unknown number of lipids could be present in the fraction of features that were unidentified.

Metabolites involved in bioenergetics processes such as cellular respiration and β-oxidation have been shown to affect embryonic development and were found in the uterus including glucose/fructose, malate, and L-canitine. None of these molecules changed over time.

TABLE 2 Metabolites reported to affect preimplantation development present in uterine horn ipsilateral to the side of ovulation within the first 7 days relative to ovulation

Mode	Mass	Time	Putative identification	Action on preimplantation development (species)
(−)	152.0	0.80	3-Sulfino-L-alanine	Increase development to blastocyst stage (rats)[a]
(−)	215.0	0.71	Glucose/fructose	Phosphorylates mTORC1 and ribosomal S6 kinase[a] (rabbit)[b]; increased reactive oxygen species (mouse)[c]
(−)	217.0	0.71	Glucose/fructose	Phosphorylates mTORC1 and ribosomal S6 kinase[a] (rabbit)[b]; increased reactive oxygen species (mouse)[c]
(−)	133.0	1.04	Malate	Improve development to 8-cell stage (hamster)[d]
(−)	133.0	1.19	Malate	Improve development to 8-cell stage (hamster)[d]
(−)	116.0	1.16	N-Acetylglycine	Increase development to blastocyst stage (rats)[a]
(−)	116.0	1.16	N-Acetylglycine	Increase development to blastocyst stage (rats)[a]
(−)	160.1	0.89	N-Methyl-L-glutamate	Increase development to blastocyst stage (rats)[a]
(−)	124.0	0.71	Taurine	Increased embryo viability (bovine)[e]; increase development to blastocyst stage (rats)[a]
(+)	157.0	0.98	(R)-Malate	Improve development to 8-cell stage (hamster)[d]
(+)	132.1	0.77	5-Aminolevulinic acid	Impaired development to the blastocyst stage (mouse)[f]
(+)	137.0	6.07	Allopurinol	Inhibits morula and blastocyst formation (rabbit)[g]
(+)	391.3	16.57	Bis(2-ethylhexyl) phthalate	Impaired development to the blastocyst stage (mouse)[h]
(+)	279.2	14.66	Dibutyl phthalate	Impaired development to the blastocyst stage (mouse)[h]
(+)	162.1	0.94	L-Carnitine	Decrease size of lipid bodies (mice)[i]; increased rate of ATP:ADP conversion (bovine)[j]
(+)	132.1	2.51	Leucine	Altered gene expression in mTORC dependent manner (rabbit)[b]
(+)	132.1	2.24	Leucine	Regulated TE motility (mouse)[k]
(+)	150.1	1.62	L-Methionine	Increase lipid accumulation and reduces methylation (bovine)[l]
(+)	223.1	12.40	Monobutyl phthalate	Impaired development to the blastocyst stage (mouse)[h]
(+)	126.0	0.71	Taurine	Increased embryo viability (bovine)[e]; increase development to blastocyst stage (rats)[a]

[a]Nakamura et al. (2016).
[b]Gürke et al. (2016).
[c]Nasr-Esfahani and Johnson (1991).
[d]Ain and Seshagiri (1997).
[e]Ealy et al. (1992).
[f]Yang, Greer, Van Vugt, and Reid (1995).
[g]Miyazaki, Kuo, Dharmarajan, Atlas, and Wallach (1989).
[h]Chu et al. (2013).
[i]Kyvelidou et al. (2016).
[j]Sutton-McDowall, Feil, Robker, Thompson, and Dunning (2012).
[k]González et al. (2012).
[l]Acosta et al. (2016).

Two very abundant metabolites were hippuric acid and *p*-cresol sulfate. Although these two metabolites are typically observed in urine, they are also present in several other fluids (Dame et al., 2015; Kolho, Pessia, Jaakkola, de Vos, & Velagapudi, 2017) and circulate in blood plasma (Hoffmann, Meier-Augenstein, Stöckler, Surtees, & Nyhan, 1993). Their presence in uterine flushings probably represents transudation from blood plasma. Other metabolites found were various phthalates, which were likely present because of contamination of the flush fluid from constituents in the plastic tube used for flushing.

The most common pattern of temporal change in intensity of the features was characterized by a peak on Day 5 followed by a decreased by Day 7. It is possible that this pattern represents interactions between progesterone and estrogen in their actions on endometrial function. Indeed, effects of progesterone on endometrial

secretion of proteins can be either enhanced or inhibited by estradiol (Fazleabas, Bazer, & Roberts, 1982; Hansen, Bazer, & Roberts, 1985). Perhaps actions of estrogen on the uterus at Day 5 enhance the stimulatory effect of progesterone on secretion of metabolites but the decline of estrogen influence by Day 7 results in a lack of action of progesterone on secretion by that day.

Our data provide evidence of changes in the metabolome of the uterine fluid during the period when the embryo transitions from the morula to the blastocyst stage of development, with many metabolites reaching highest intensity between Days 5 and 7 after ovulation. Many of the metabolites found in the uterus are known to regulate cell signaling or have been reported to affect embryonic development. These may be important molecules for future studies aiming to characterize the maternal microenvironment of preimplantation embryos; the first step toward a systematic

characterization of maternal secretions involved in regulation of embryonic development.

CONFLICTS OF INTEREST

The authors declare that there are no conflicts of interest.

ORCID

Peter J. Hansen http://orcid.org/0000-0003-3061-9333

REFERENCES

Aberdeen, G. W., Wiegand, S. J., Bonagura, T. W., Jr., Pepe, G. J., & Albrecht, E. D. (2008). Vascular endothelial growth factor mediates the estrogen-induced breakdown of tight junctions between and increase in proliferation of microvessel endothelial cells in the baboon endometrium. *Endocrinology, 149,* 6076–6083.

Acosta, D. A. V., Denicol, A. C., Tribulo, P., Rivelli, M. I., Skenandore, C., Zhou, Z., ... Cardoso, F. C. (2016). Effects of rumen-protected methionine and choline supplementation on the preimplantation embryo in Holstein cows. *Theriogenology, 85,* 1669–1679.

Ain, R., & Seshagiri, P. B. (1997). Succinate and malate improve development of hamster eight-cell embryos in vitro: Confirmation of viability by embryo transfer. *Molecular Reproduction and Development, 47,* 440–447.

Albrecht, E. D., Aberdeen, G. W., Niklaus, A. L., Babischkin, J. S., Suresch, D. L., & Pepe, G. J. (2003). Acute temporal regulation of vascular endothelial growth/permeability factor expression and endothelial morphology in the baboon endometrium by ovarian steroids. *Journal of Clinical Endocrinology and Metabolism, 88,* 2844–2852.

Amaro, I. R., Vicente-Villardón, J. L., & Galindo-Villardón, M. P. (2004). Manova Biplot para arreglos de tratamientos con dos factores basado en modelos lineales generales multivariantes. *Interciencia, 29,* 26–32.

Belaz, K. R. A., Tata, A., Franca, M. R., Santos da Silva, M. I., Vendramini, P. H., Fernandes, A. M. A. P., ... Binelli, M. (2016). Phospholipid profile and distribution in the receptive oviduct and uterus during early diestrus in cattle. *Biology of Reproduction, 95,* 127–127.

Bollwein, H., Prost, D., Ulbrich, S. E., Niemann, H., & Honnens, A. (2010). Effects of a shortened preovulatory follicular phase on genital blood flow and endometrial hormone receptor concentrations in Holstein-Friesian cows. *Theriogenology, 73,* 242–249.

Chu, D. P., Tian, S., Sun, D. G., Hao, C. J., Xia, H. F., & Ma, X. (2013). Exposure to mono-n-butyl phthalate disrupts the development of preimplantation embryos. *Reproduction, Fertility, and Development, 25,* 1174–1184.

Dame, Z. T., Aziat, F., Mandal, R., Krishnamurthy, R., Bouatra, S., Borzouie, S., ... Wishart, D. S. (2015). The human saliva metabolome. *Metabolomics, 11,* 1864–1883.

Ealy, A., Drost, M., Barros, C., & Hansen, P. (1992). Thermoprotection of preimplantation bovine embryos from heat shock by glutathione and taurine. *Cell Biology International Reports, 16,* 125–131.

Elhassan, Y. M., Wu, G., Leanez, A. C., Tasca, R. J., Watson, A. J., & Westhusin, M. E. (2001). Amino acid concentrations in fluids from the bovine oviduct and uterus and in KSOM-based culture media. *Theriogenology, 55,* 1907–1918.

Fahning, M. L., Schultz, R. H., & Graham, E. F. (1967). The free amino acid content of uterine fluids and blood serum in the cow. *Journal of Reproduction and Fertility, 13,* 229–236.

Fazleabas, A. T., Bazer, F. W., & Roberts, R. M. (1982). Purification and properties of a progesterone-induced plasmin/trypsin inhibitor from uterine secretions of pigs and its immunocytochemical localization in the pregnant uterus. *Journal of Biological Chemistry, 257,* 6886–6897.

Forde, N., Simintiras, C. A., Sturmey, R., Mamo, S., Kelly, A. K., Spencer, T. E., ... Lonergan, P. (2014). Amino acids in the uterine luminal fluid reflects the temporal changes in transporter expression in the endometrium and conceptus during early pregnancy in cattle. *PLOS One, 9,* e100010.

França, M. R., da Silva, M. I. S., Pugliesi, G., Van Hoeck, V., & Binelli, M. (2017). Evidence of endometrial amino acid metabolism and transport modulation by peri-ovulatory endocrine profiles driving uterine receptivity. *Journal of Animal Science and Biotechnology, 8,* 54.

Goddard, L. M., Murphy, T. J., Org, T., Enciso, J. M., Hashimoto-Partyka, M. K., Warren, C. M., ... Iruela-Arispe, M. L. (2014). Progesterone receptor in the vascular endothelium triggers physiological uterine permeability preimplantation. *Cell, 156,* 549–562.

González, I. M., Martin, P. M., Burdsal, C., Sloan, J. L., Mager, S., Harris, T., & Sutherland, A. E. (2012). Leucine and arginine regulate trophoblast motility through mTOR-dependent and independent pathways in the preimplantation mouse embryo. *Developmental Biology, 361,* 286–300.

Gürke, J., Schindler, M., Pendzialek, S. M., Thieme, R., Grybel, K. J., Heller, R., ... Navarrete santos, A. (2016). Maternal diabetes promotes mTORC1 downstream signaling in rabbit preimplantation embryos. *Reproduction, 151,* 465–476.

Hackett, A. J., Durnford, R., Mapletoft, R. J., & Marcus, G. J. (1993). Location and status of embryos in genital tract of superovulated cows 4 to 6 days after insemination. *Theriogenology, 40,* 1147–1153.

Hansen, P. J., Bazer, F. W., & Roberts, R. M. (1985). Appearance of β-hexosaminidase and other lysosomal-like enzymes in the uterine lumen of gilts, ewes and mares in response to progesterone and oestrogens. *Journal of Reproduction and Fertility, 73,* 411–424.

Hansen, P. J., Block, J., Loureiro, B., Bonilla, L., & Hendricks, K. E. M. (2010). Effects of gamete source and culture conditions on the competence of in vitro-produced embryos for post-transfer survival in cattle. *Reproduction, Fertility, and Development, 22,* 59–66.

Hata, M., Yamanegi, K., Yamada, N., Ohyama, H., Yukitatsu, Y., Nakasho, K., ... Terada, N. (2014). Estrogen decreases the expression of claudin-5 in vascular endothelial cells in the murine uterus. *Endocrine Journal, 61,* 705–715.

Hawk, H. W. (1983). Sperm survival and transport in the female reproductive tract. *Journal of Dairy Science, 66,* 2645–2660.

Hoffmann, G. F., Meier-Augenstein, W., Stöckler, S., Surtees, R., Rating, D., & Nyhan, W. L. (1993). Physiology and pathophysiology of organic acids in cerebrospinal fluid. *Journal of Inherited Metabolic Disease, 16,* 648–669.

Honnens, A., Voss, C., Herzog, K., Niemann, H., Rath, D., & Bollwein, H. (2008). Uterine blood flow during the first 3 weeks of pregnancy in dairy cows. *Theriogenology, 70,* 1048–1056.

Hugentobler, S. A., Diskin, M. G., Leese, H. J., Humpherson, P. G., Watson, T., Sreenan, J. M., & Morris, D. G. (2007). Amino acids in

oviduct and uterine fluid and blood plasma during the estrous cycle in the bovine. *Molecular Reproduction and Development*, 74, 445–454.

Hugentobler, S. A., Sreenan, J. M., Humpherson, P. G., Leese, H. J., Diskin, M. G., & Morris, D. G. (2010). Effects of changes in the concentration of systemic progesterone on ions, amino acids and energy substrates in cattle oviduct and uterine fluid and blood. *Reproduction, Fertility and Development*, 22, 684–694.

Jørgensen, E., & Pedersen, A. R. (1998). *How to obtain those nasty standard errors from transformed data and why they should not be used* (Report 7), Aarhus, Denmark: Danish Institute of Agricultural Biometry Research.

Katila, T. (2012). Post-mating inflammatory responses of the uterus. *Reproduction in Domestic Animals*, 47, 31–41.

Kolho, K. L., Pessia, A., Jaakkola, T., de Vos, W. M., & Velagapudi, V. (2017). Faecal and serum metabolomics in paediatric inflammatory bowel disease. *Journal of Crohn's & Colitis*, 11, 321–334.

Koos, R. D. (2011). Minireview: Putting physiology back into estrogens mechanism of action. *Endocrinology*, 152, 4481–4488.

Krzanowski, W. J. (1989). On confidence regions in canonical variate analysis. *Biometrika*, 76, 107–116.

Kyvelidou, C., Sotiriou, D., Antonopoulou, T., Tsagkaraki, M., Tserevelakis, G. J., Filippidis, G., & Athanassakis, I. (2016). L-Carnitine affects preimplantation embryo development toward infertility in mice. *Reproduction*, 152, 283–291.

Malayer, J. R., Hansen, P. J., & Buhi, W. C. (1988). Effect of day of the oestrous cycle, side of the reproductive tract and heat shock on in-vitro protein secretion by bovine endometrium. *Journal of Reproduction and Fertility*, 84, 567–578.

McRae, A. C. (1988). The blood-uterine lumen barrier and exchange between extracellular fluids. *Journal of Reproduction and Fertility*, 82, 857–873.

Mitko, K., Ulbrich, S. E., Wenigerkind, H., Sinowatz, F., Blum, H., Wolf, E., & Bauersachs, S. (2008). Dynamic changes in messenger RNA profiles of bovine endometrium during the oestrous cycle. *Reproduction*, 135, 225–240.

Miyazaki, T., Kuo, T. C., Dharmarajan, A. M., Atlas, S. J., & Wallach, E. E. (1989). In vivo administration of allopurinol affects ovulation and early embryonic development in rabbits. *American Journal of Obstetrics and Gynecology*, 161, 1709–1714.

Nakamura, K., Morimoto, K., Shima, K., Yoshimura, Y., Kazuki, Y., Suzuki, O., … Ohbayashi, T. (2016). The effect of supplementation of amino acids and taurine to modified KSOM culture medium on rat embryo development. *Theriogenology*, 86, 2083–2090.

Nasr-Esfahani, M. H., & Johnson, M. H. (1991). The origin of reactive oxygen species in mouse embryos cultured in vitro. *Development*, 113, 551–561.

Pluskal, T., Castillo, S., Villar-Briones, A., & Orešič, M. (2010). MZmine 2: Modular framework for processing, visualizing, and analyzing mass spectrometry- based molecular profile data. *BMC Bioinformatics*, 11, 395.

Ribeiro, E. S., Gomes, G., Greco, L. F., Cerri, R. L. A., Vieira-Neto, A., Monteiro, P. L. J., … Santos, J. E. P. (2016). Carryover effect of postpartum inflammatory diseases on developmental biology and fertility in lactating dairy cows. *Journal of Dairy Science*, 99, 2201–2220.

Romero, J. J., Liebig, B. E., Broeckling, C. D., Prenni, J. E., & Hansen, T. R. (2017). Pregnancy-induced changes in metabolome and proteome in ovine uterine flushings. *Biology of Reproduction*, 97, 273–287.

Roussel, J. D., & Loe, W. C. (1973). Effects of heat stress and melengestrol acetate on amino acid pattern of uterine fluid from dairy heifers. *International Journal of Biometeorology*, 17, 153–156.

Roy, V. K., & Krishna, A. (2013). Changes in glucose and carnitine levels and their transporters in utero-tubal junction in relation to sperm storage in the vespertilionid bat, *Scotophilus heathi*. *Journal of Experimental Zoology Part A*, 319, 517–526.

Schuberth, H. J., Taylor, U., Zerbe, H., Waberski, D., Hunter, R., & Rath, D. (2008). Immunological responses to semen in the female genital tract. *Theriogenology*, 70, 1174–1181.

Schultz, R. H., Fahning, M. L., & Graham, E. F. (1971). A chemical study of uterine fluid and blood serum of normal cows during the oestrous cycle. *Journal of Reproduction and Fertility*, 27, 355–367.

Sutton-McDowall, M. L., Feil, D., Robker, R. L., Thompson, J. G., & Dunning, K. R. (2012). Utilization of endogenous fatty acid stores for energy production in bovine preimplantation embryos. *Theriogenology*, 77, 1632–1641.

Tríbulo, P., Siqueira, L. G. B., Oliveira, L. J., Scheffler, T., & Hansen, P. J. (2018). Identification of potential embryokines in the bovine reproductive tract. *Journal of Dairy Science*, 101, 690–704.

Ulmer, C. Z., Yost, R. A., Chen, J., Mathews, C. E., & Garrett, T. J. (2015). Liquid chromatography-mass spectrometry metabolic and lipidomic sample preparation workflow for suspension-cultured mammalian cells using Jurkat T lymphocyte cells. *Journal of Proteomics and Bioinformatics*, 8, 126–132.

Wira, C. R., Fahey, J. V., Rodriguez-Garcia, M., Shen, Z., & Patel, M. V. (2014). Regulation of mucosal immunity in the female reproductive tract: The role of sex hormones in immune protection against sexually transmitted pathogens. *American Journal of Reproductive Immunology*, 72, 236–258.

Xia, J., Wishart, D. S. (2016). Using MetaboAnalyst 3.0 for comprehensive metabolomics data analysis. *Curr Protoc Bioinformatics*. 7;55:14.10.1-14.10.91. https://doi.org/10.1002/cpbi.11

Yang, J. Z., Greer, P. A., Van Vugt, D. A., & Reid, R. L. (1995). Treatment with 5-aminolevulinic acid and photoactivating light causes destruction of preimplantation mouse embryos. *Fertility and Sterility*, 63, 1088–1093.

SUPPORTING INFORMATION

Additional supporting information may be found online in the Supporting Information section at the end of the article.